

Supplementary Information

Accelerated Fenton-like kinetics by visible-light-driven catalysis over Iron(III) porphyrin functionalized Zirconium MOF: Effective promotion on the degradation of organic contaminant

Lei Wang,^{a,c} Pengxia Jin,^a Shuhua Duan,^a Jingwei Huang,^{a,b} Houde She,^a Qizhao Wang,^{*a,c} and Taicheng An^{*b}

^a Research Center of Gansu Military and Civilian Integration Advanced Structural Materials, College of Chemistry and Chemical Engineering, Northwest Normal University, Lanzhou 730070, China

^b Guangzhou Key Laboratory of Environmental Catalysis and Pollution Control, School of Environmental Science and Engineering, Institute of Environmental Health and Pollution Control, Guangdong University of Technology, Guangzhou, 510006, China

^c Key Laboratory for Photonic and Electronic Bandgap Materials, Ministry of Education, School of Physics and Electronic Engineering, Harbin Normal University, Harbin 150025, China

*Corresponding author. Tel: +86 931 7972677; Fax: +86 931 7972677.

*Corresponding author.

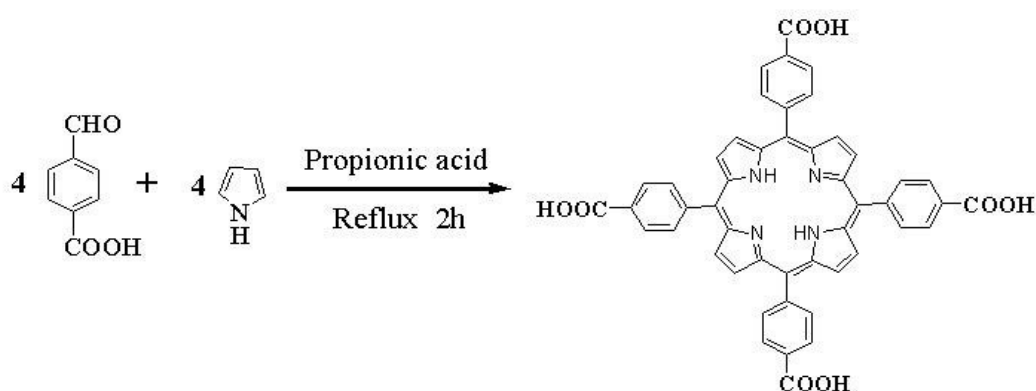
E-mail: wangqizhao@163.com(Q.Wang); antc99@gdut.edu.cn(T. An)

Section S1. Materials

Pyrrrole (Adamas Reagent Co., Ltd, 99.0%), 4-formylbenzoic acid (Adamas Reagent Co., Ltd, 99.0%) and propionic acid (Adamas Reagent Co., Ltd, 99.0%) were purchased from Damas-beta. Benzoic acid ($C_7H_6O_2$, 99.9%), rhodamine B (RhB), tert-butanol (TBA), ammonium oxalate (AO), p-benzoquinone (BQ), iron(II) chloride tetrahydrate ($FeCl_2 \cdot 4H_2O$), zirconium(IV) chloride ($ZrCl_4$, 98%) and terephthalic acid ($C_8H_6O_4$, BDC, 98%) were provided by Sinopharm Chemical Reagent Co. Ltd. N,N-dimethylformamide (C_3H_7NO , DMF, 99.9%), ethanol and acetone were supplied by Sinopharm Chemical Reagent Co. Ltd. Hydrochloric acid (HCl, 36%-38%), hydrofluoric acid (HF, $\geq 40\%$), Sulfuric acid (H_2SO_4 , 98%), H_2O_2 (30wt%) and nitric acid (HNO_3 , 65%-68%) were of analytical grade and bought from Medicines Corporation Ltd. China National. Chemical oxygen demand (COD) special consumable reagent (LH-D/E-100) were purchased from Lanzhou Lianhua Environmental Protection Technology Co. Ltd. Except pyrrole, which was purified by distillation under reduced pressure before each used, all reagents are of analytical grade and used without further purification. Analytical grade water was provided by Millipore Elix 3 system combined to a prograd filter (Millipore AG, Zug, Switzerland Lab Ultra-pure Water Purification equipment-HYJD). Glassware for analytical analyses and reactions were acid soaked after every experimental workup in order to prevent iron cross-contamination (10% HCl, 3 days and nights).

Section S2. Preparation of tetrakis(4-carboxyphenyl)-porphyrin (TCPP) and tetrakis(4-phenyl)porphyrin (TPP)

Porphyrin was prepared according to previous report.^[1] To the solution of 4-formylbenzoic acid (3.04 g, 20.25 mmol) and pyrrole (1.4 g, 20.25 mmol), 75 mL propionic acid was added and then refluxed for 2 h. After cooling down to room temperature, the engendered black solution was diluted with 80 mL methanol before subsequently stirring for 0.5 h in ice bath. The blend was centrifuged, and afterwards washed with methanol and warmed pure water for more than 3 times. The generated precipitate was further dried in an oven at 80°C for 12 h to give the targeted purple powders, TCPP (Yield: 18%) (Scheme S1). ¹H-NMR (600 MHz, DMSO-*d*₆, ppm): δ 8.79 (s, 8H); 8.33(d, 8H); 8.26 (d, 8H); UV-vis (alcohol): λ_{max}/nm 413 (Soret band) and 518, 555, 580, 635 (Q bands); FT-IR (KBr): ν_{max}/cm⁻¹ 3315, 965 (N-H) (Fig. S1-2 and Fig. S4).



Scheme S1. Synthesis route of TCPP compound.

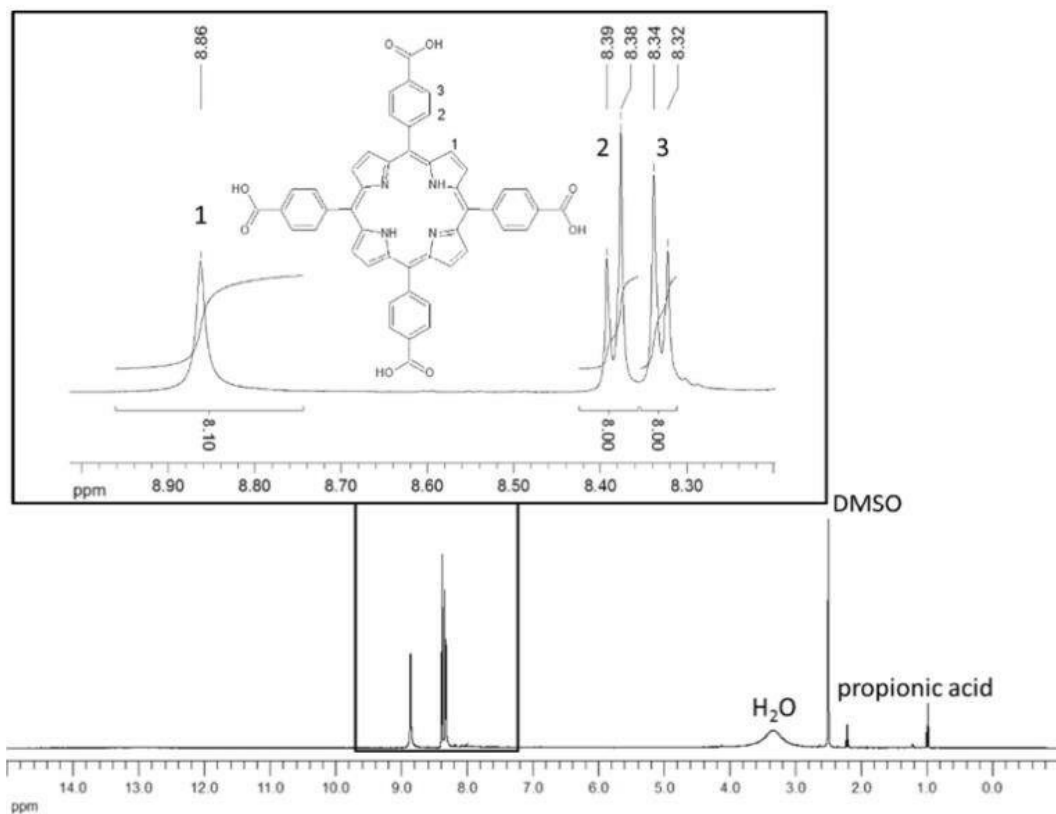
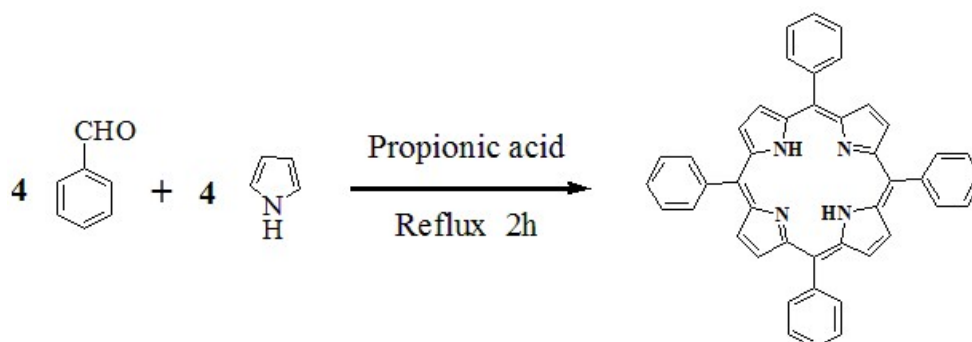


Fig. S1. $^1\text{H-NMR}$ spectrum of the synthesized TCPP linker.

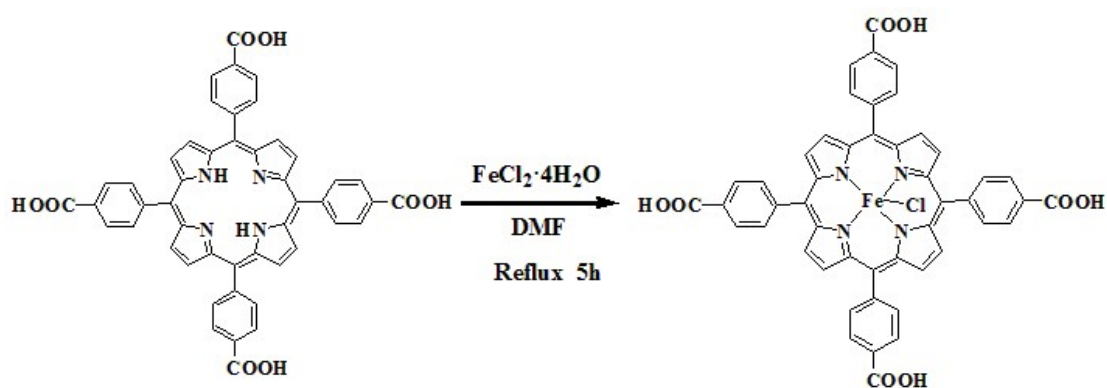
The synthetic procedure of TPP is analogous to the process above except for the substitution of benzaldehyde for the reactant 4-formylbenzoic acid (Scheme S2). $^1\text{H-NMR}$ (600 MHz, $\text{DMSO-}d_6$, ppm): δ 8.83 (s, 8H); 8.22 (d, 8H); 7.83 (d, 8H).



Scheme S2. Synthesis route of TPP compound.

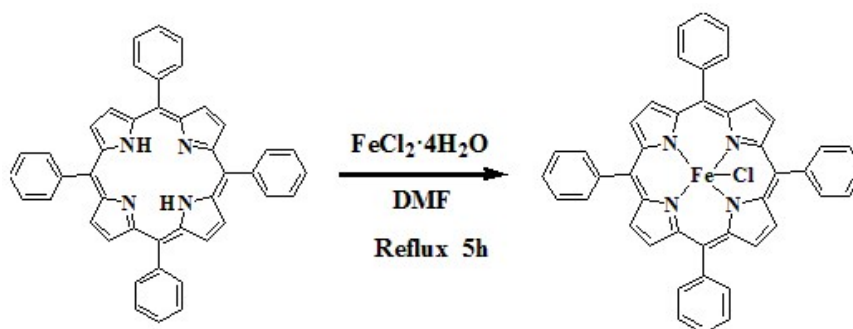
Section S3. Preparation of [5, 10, 15, 20-tetrakis(4-carboxylphenyl)porphyrinato]-Fe(III) chloride (Fe^{III}-TCPPCl) and tetrakis(4-phenyl)porphyrin-Fe(III) (Fe^{III}-TPPCL)

Iron(III) meso-tetra(4-carboxyphenyl) porphyrin complex was prepared following a published procedure.^[2] 15 mL DMF was employed to dissolve TCPP (0.261 g, 0.33 mmol) as well as FeCl₂·4H₂O (0.31 g, 1.82 mmol), and the solution was kept refluxing for 5 h. After the brown solution was cooled to room temperature, the mixture was centrifuged to separate out the precipitate, which was washed with pure water for more than 5 times. The obtained solid was further dried in vacuum oven at 60 °C for 12 h to give a brown solid as targeted product (Yield: 53.4%). (Scheme S3). UV-vis (alcohol): λ_{max}/nm 416 (Soret band) and 517, 570, 611 (Q bands); FT-IR (KBr): ν_{max}/cm⁻¹ 1000 (Fe-N). (Fig. S1b, 3a).



Scheme S3. Synthesis of Fe^{III}-TCPPCl metallic compound.

The preparation of Fe^{III}-TPPCl is similar to the procedure above except for that the mixed ligand was replaced by tetrakis(4-phenyl)porphyrin (Scheme S4).

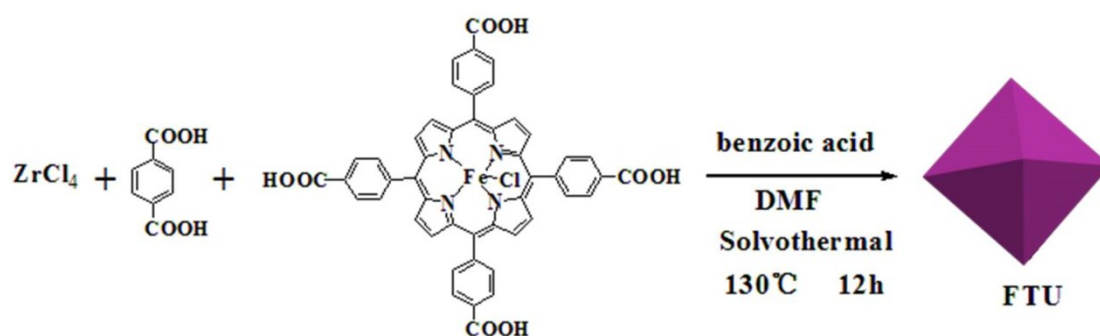


Scheme S4. Synthesis of Fe^{III}-TPPCl metallic compound.

Section S4. Preparation of Fe^{III}-TCPPCl⊂UiO-66 (FTU), TCPP⊂UiO-66 (TU) and Fe^{III}-TPPCl⊂UiO-66

Typically, FTU was solvothermally synthesized due to the published literature.^[3] ZrCl₄ (0.03 g, 0.129 mmol), BDC (0.03 g, 0.181 mmol), Fe^{III}-TCPPCl (0.01 g, 0.011 mmol) and benzoic acid (0.5 g, 4.098 mmol) were mixed in 2.0 mL DMF. After vigorously stirring for 30 min, the mixture was poured into 50 ml teflon-lined steel autoclave and subsequently heated at 130°C for 12 h. After cooling down to room temperature, centrifugation of the mixture gave a brown solid. To remove unreacted precursors, the solid was washed with DMF and acetone more than 3 times. The generated brown powder was centrifuged and subsequently dried in an oven at 80

°C for 12 h to give targeted product (Scheme. S5). The synthesis of UiO-66 was similar to the procedure given above, except for the absence of Fe^{III}-TCPPCl. With respect to the preparation of TCPP@UiO-66 or Fe^{III}-TCPPCl@UiO-66, the synthetic route was analogous to the preparation process mentioned above, except for that Fe^{III}-TCPPCl was substituted by TCPP or Fe^{III}-TPPCL.



Scheme S5. Synthesis of FTU.

Section S5. UV-vis absorption spectrum in ethanol solution

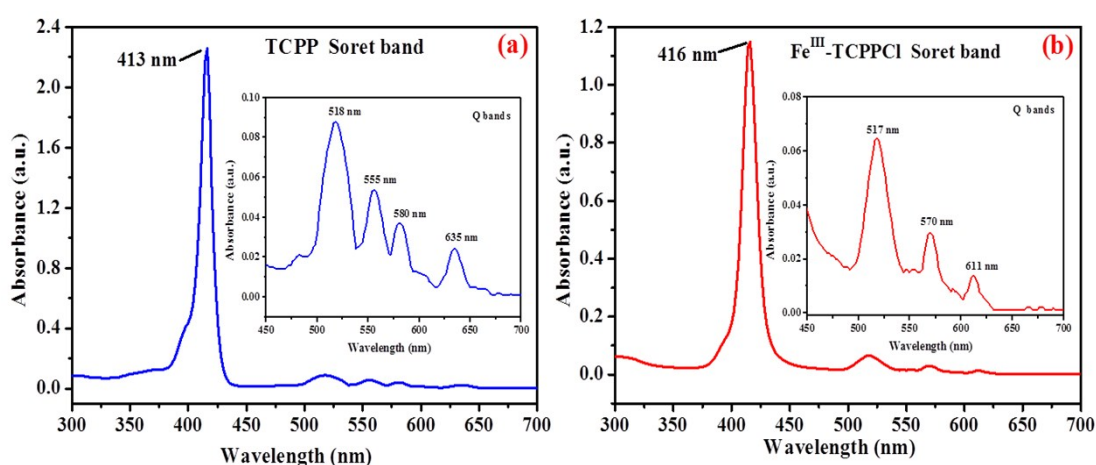


Fig. S2. UV-vis spectra of (a) TCPP and (b) Fe^{III}-TCPPCl dissolved in ethanol solution.

Section S6. SEM image, HAADF-STEM and elemental mapping analysis

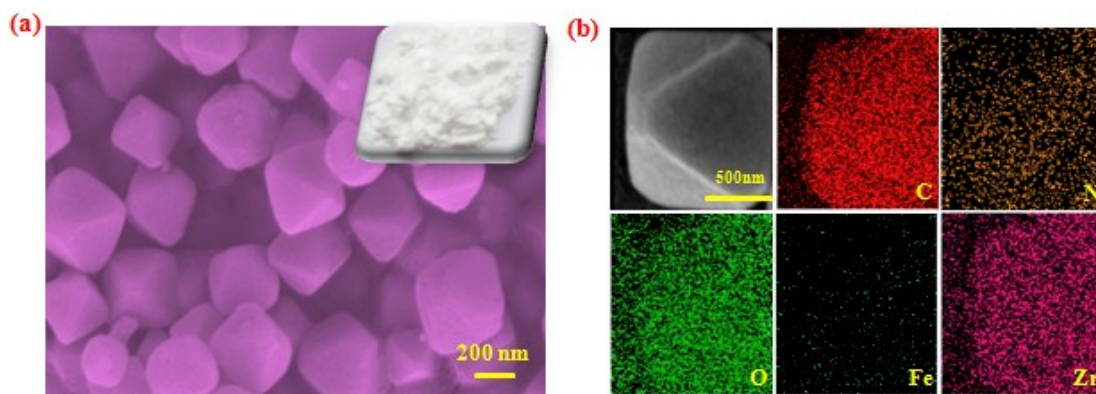


Fig. S3. (a) SEM image of UiO-66 single crystal (Scale bar: 200 nm) (the internal illustrations are photographs of UiO-66); (b) HAADF-STEM and elemental mapping analysis of FTU composite.

Section S7. FT-IR spectra

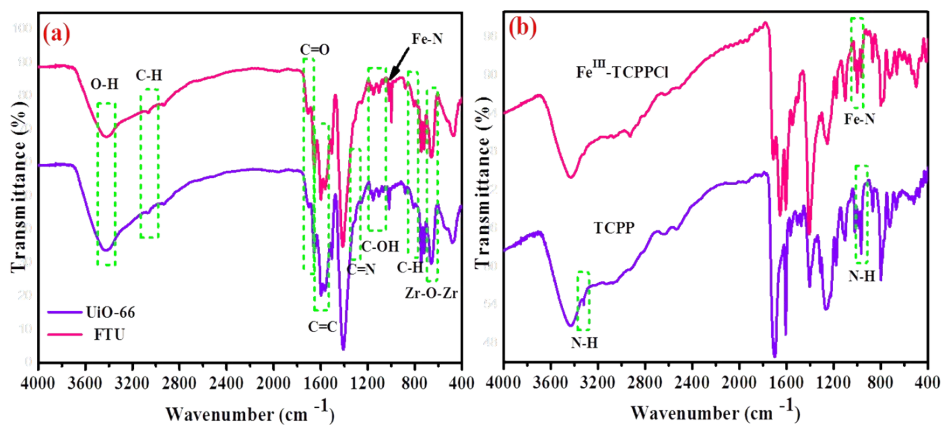


Fig. S4. FT-IR spectra: (a) UiO-66 and FTU; (b) TCPP and Fe^{III}-TCPPCl.

Section S8. XPS survey spectra

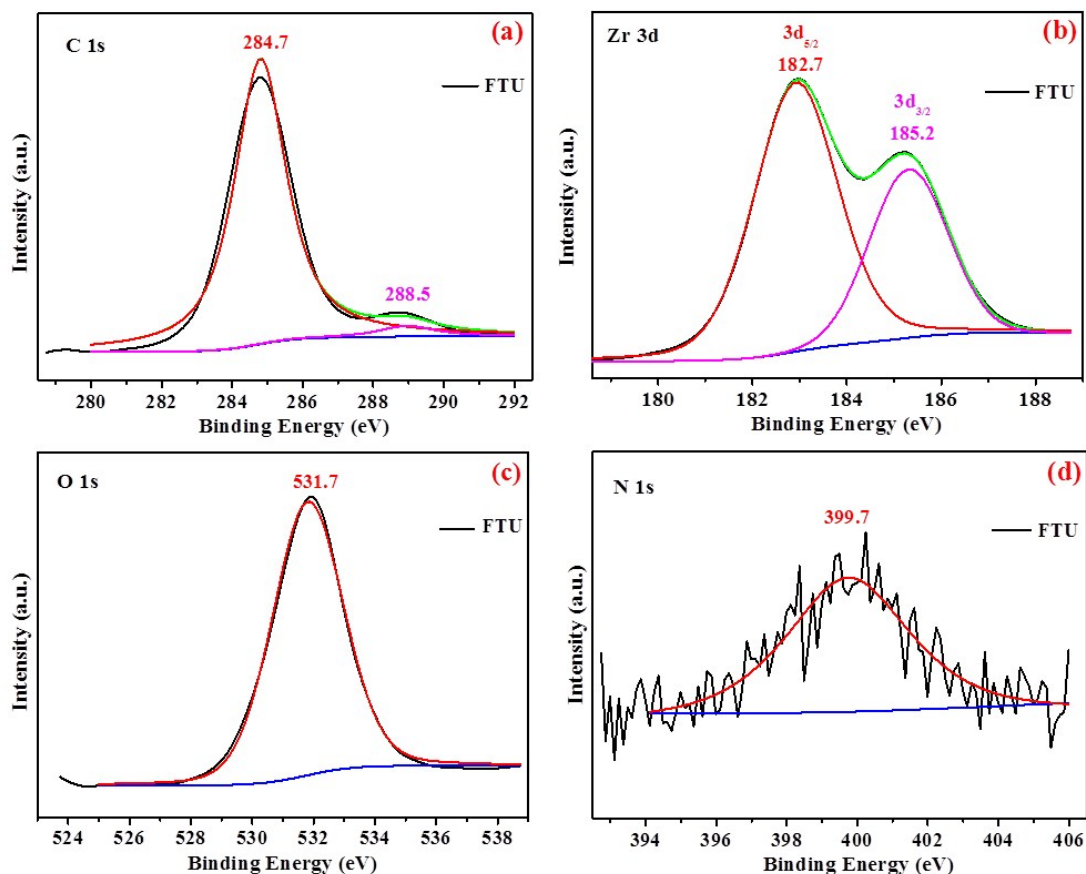


Fig. S5. XPS survey spectra of FTU: (a) C 1s for FTU; (b) Zr 3d for FTU ; (c) O 1s for FTU and (d) N 1s for FTU.

Section S9. Preparation of post-modified UiO-66 by Fe^{III}-TCPPCI (PMU)

The as-prepared UiO-66 was mixed with Fe^{III}-TCPPCI (10.0 mg, 0.012 mmol) in 10 mL DMF and stirred at room temperature for 12 h. The received blend was centrifuged and then thoroughly washed with pure water to remove remaining Fe^{III}-TCPPCI to give the final product.

Section S10. Digestion method of FTU and PMU

Typically, approximate 30.0 mg of dried MOF sample was digested in 5 mL 16% HF solution. The tube was then immersed in boiling water to evaporate the solution. The dried product was dissolved in DMSO- d_6 for ^1H NMR test.

Section S11. Photographs of the as-prepared samples

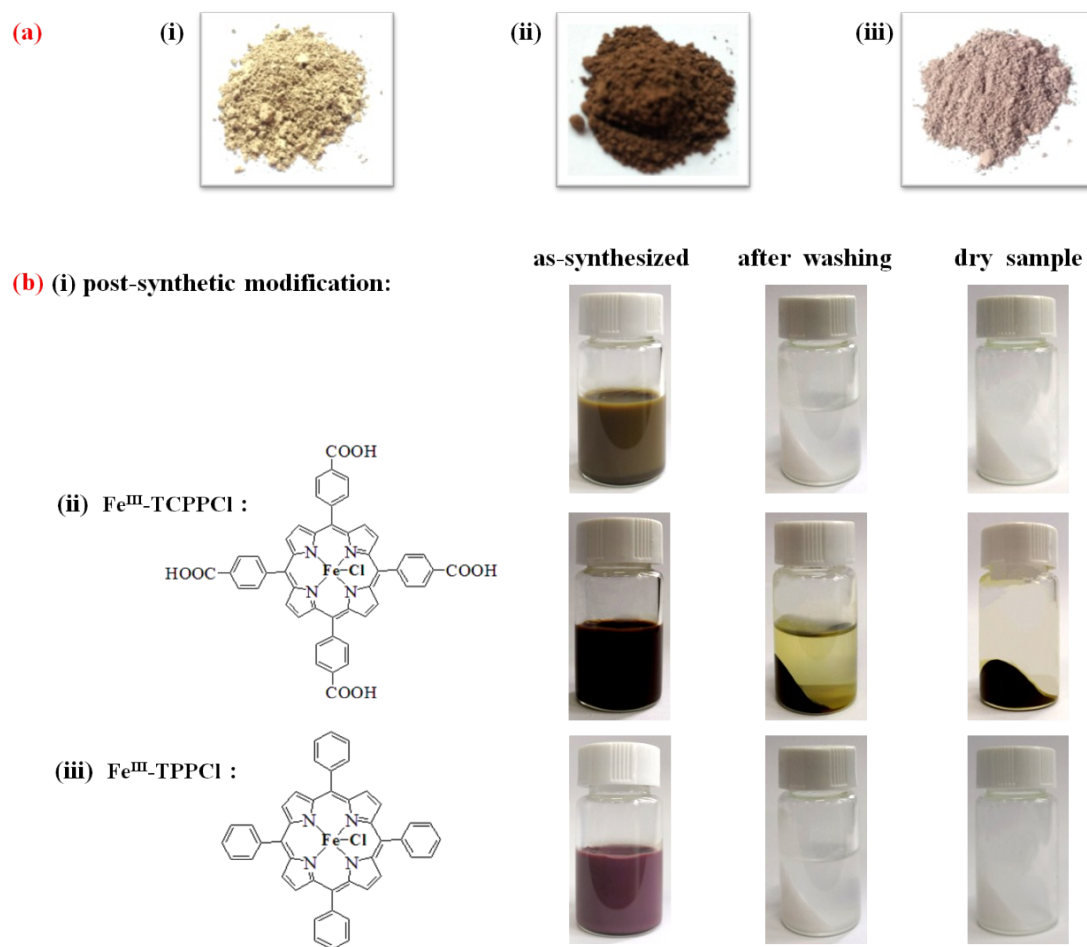


Fig. S6. (a) Photograph of different MOF powders: i) PMU, ii) FTU and iii) Fe^{III} -TPPCL-UiO-66; (b) Photographs of the solution dispersed with the MOFs under different situations: i) PMU, ii) FTU and iii) Fe^{III} -TPPCL-UiO-66.

Section S12. ^1H NMR of PMU (600 MHz, DMSO- d_6).

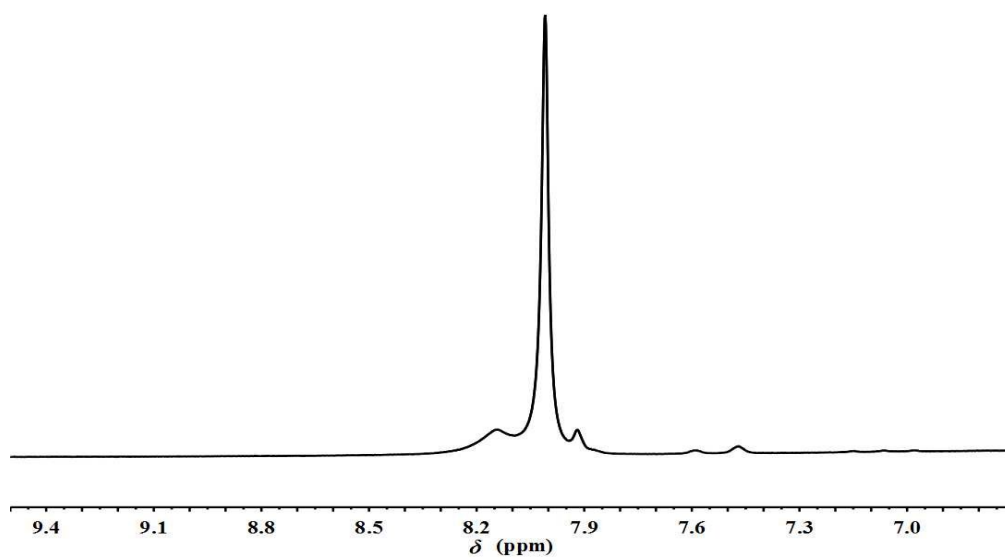


Fig. S7. ¹H NMR spectrum of the digested products from PMU: the characteristic peaks of BDC can be observed, but undetectable featured signals of Fe^{III}-TCPPCl are found.

Section S13. ¹H NMR of FTU (600 MHz, DMPO-*d*₆).

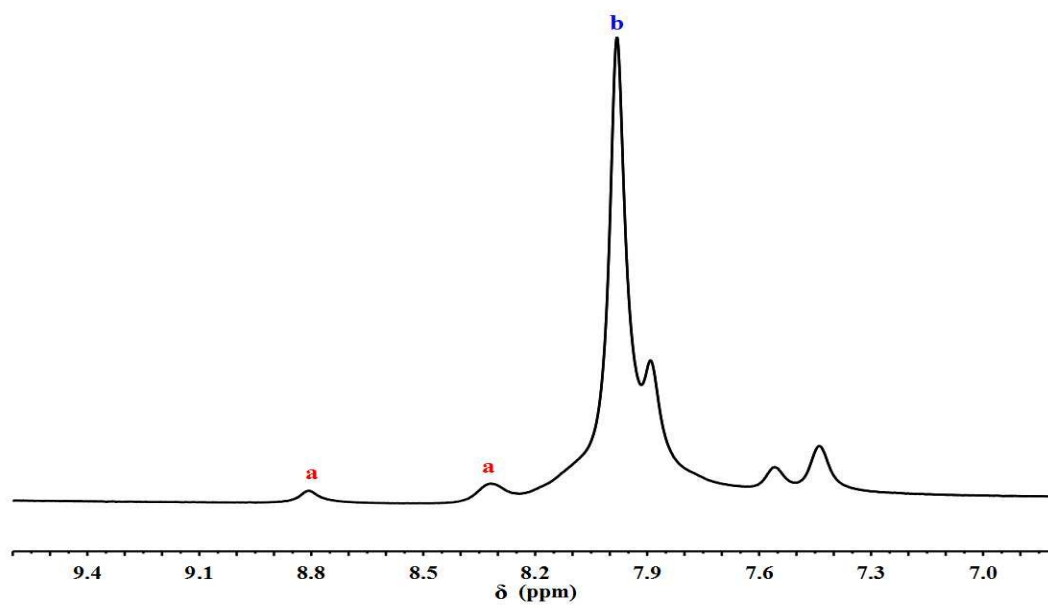


Fig. S8. ¹H NMR spectrum of the digested products from FTU: The symbol a represents characteristic signals of Fe^{III}-TCPPCI; the symbol b represents featured signals of BDC.

BDC δ: 8.00 (s, 4H). **Fe^{III}-TCPPCI** δ: 8.32 (s, 8H), 8.80 (s, 8H).

spectra and transient photocurrent responses

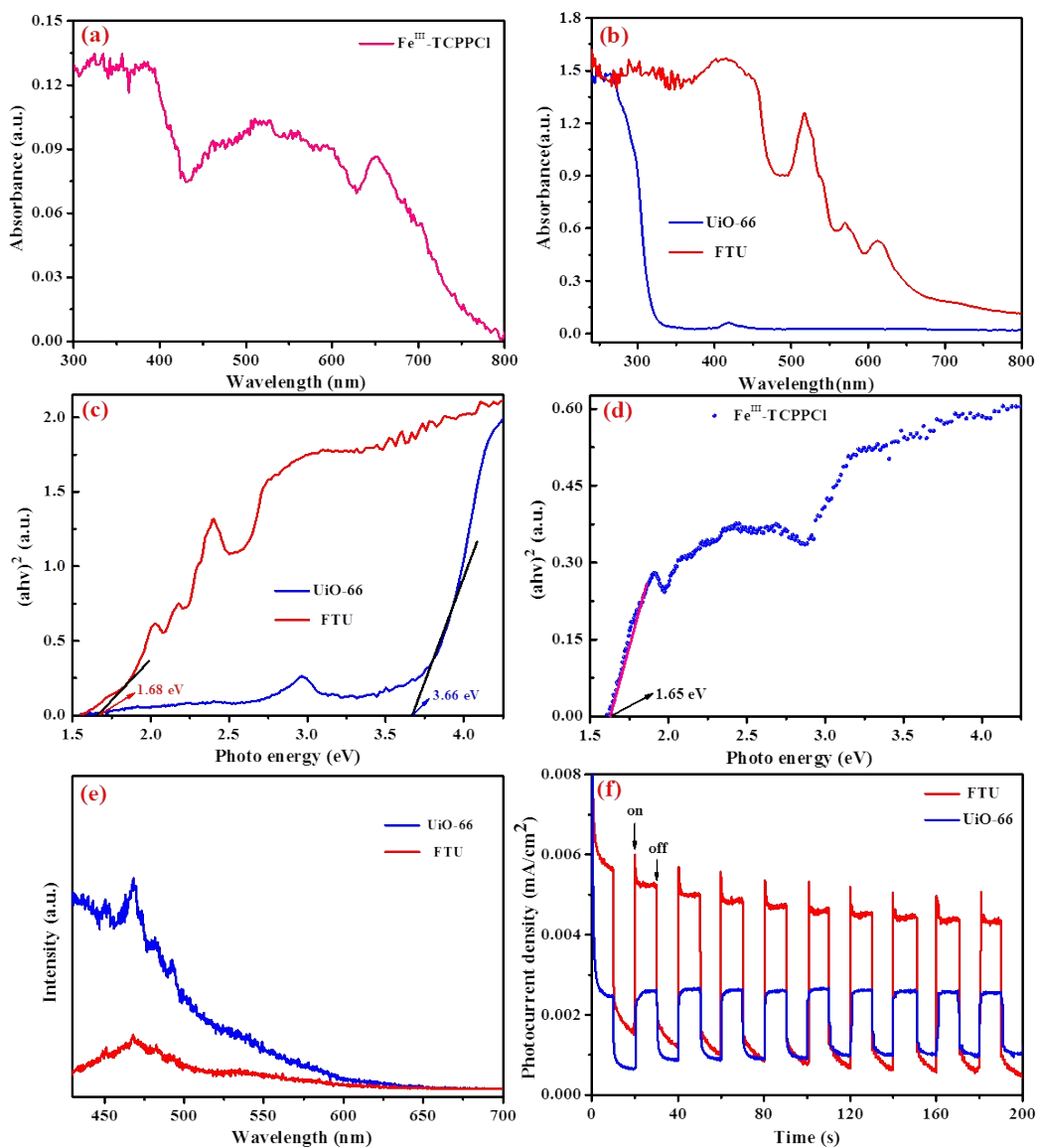


Fig. S9. (a–b) UV–vis diffuse reflectance spectra (DRS) of Fe^{III}-TCPPCI, UiO-66 and FTU. (c–d) estimation of band gap energies for UiO-66, FTU and Fe^{III}-TCPPCI. (e) PL spectra of UiO-66 and FTU; (f) Transient photocurrent responses of UiO-66 and FTU in 0.5 M Na₂SO₄ aqueous solutions under visible light irradiation.

Section S15. Mott-Schottky plots

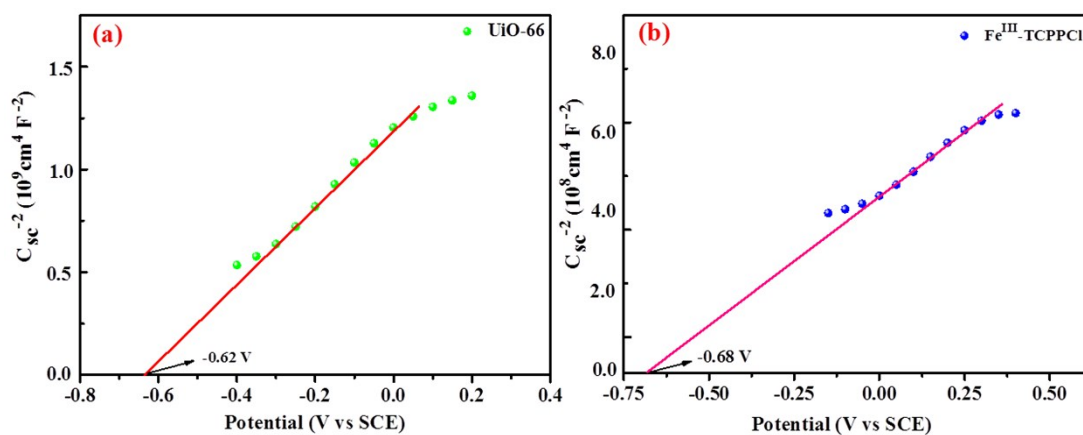


Fig. S10. Mott-Schottky plots of (a) UiO-66 and (b) Fe^{III}-TCPPCl.

Section S16. Degradation of RhB in dark system.

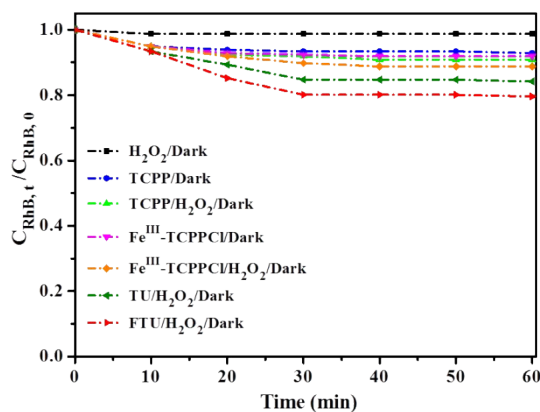
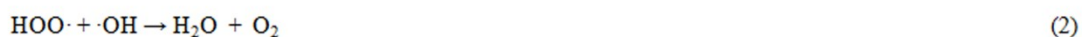


Fig. S11. Degradation of RhB by different catalysts in dark. Experimental conditions: $[C_{\text{RhB}}]_0 = 30 \text{ mg L}^{-1}$, $[\text{TCPP}, \text{Fe}^{\text{III}}\text{-TCPPCl}, \text{TU and FTU}]_0 = 0.10 \text{ g L}^{-1}$, $[\text{H}_2\text{O}_2]_0 = 2.5 \text{ mM}$, $\text{pH} = 3.5$ and temperature $= 25 \pm 2 \text{ }^\circ\text{C}$.

Section S17. Optimization of degradation conditions

Generally, Fenton-like technique is a complex system determined by many factors, all of which also correspondingly affect degradation extent of the cooperative process composed of Fenton-like reaction and photocatalysis. Therefore, prerequisite managements are required to explore the optimal reaction conditions for an utmost promotion on the removal of the pollutant. As indicated in Fig. S11, an acidic atmosphere with the optimized pH of 3.5 was selected to minimize the disadvantageous effect caused by higher pH, i.e., disproportionation of H_2O_2 into O_2 and H_2O .^[4] Note that FTU here plays dually catalytic performance in both visible-light-driven photocatalysis and Fenton-like reaction, the initial concentration of $[\text{FTU}]_0$ is also of importance. When the original H_2O_2 concentration was fixed, there is an expectedly obvious ascending trend of activity while lifting the concentration of $[\text{FTU}]_0$ from 0.05 to 0.1 g/L (Fig. S12). Continuously increasing the dosage of the catalyst, however, the resulting degradation efficiencies decreases. This attenuating trend is not merely related to the limited H_2O_2 , but owing to the fact that the excess heterogeneous catalyst would accumulate turbidity in the solution and thus reduce the visible-light penetration.^[5,6] With respect to the H_2O_2 dosage, when the concentration increased from 1.25 to 2.5 mM (Fig. S13), the degradation efficiency climbs up correspondingly from 60% to nearly 100%. Nonetheless, further increment in the dosage of H_2O_2 is not able to apparently enhance the removal efficiency. Thereby, the optimal H_2O_2 dosage was fixed as 2.5 mM since excess H_2O_2 use not only increases the cost without any promotion on the catalysis, but results in a consumption of generated hydroxyl radicals (Eqs. 1-2).^[7]



Section S18. Effect of initial pH

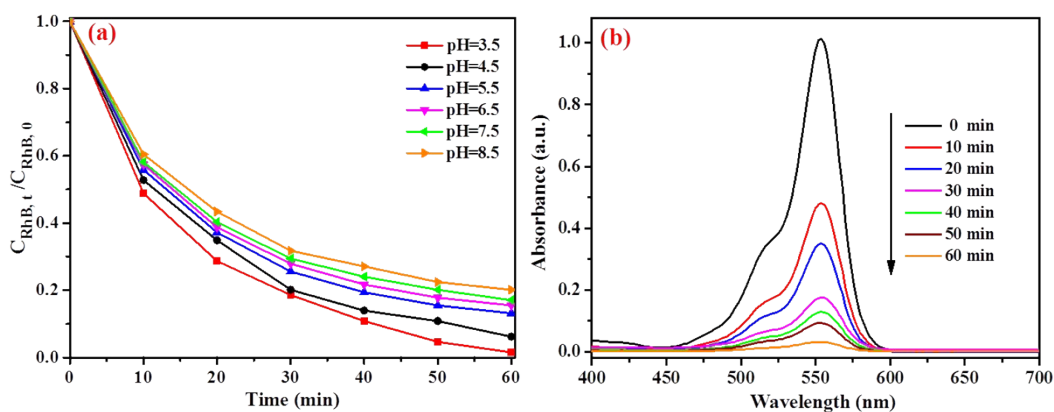


Fig. S12. (a) Effect of initial pH on the degradation of RhB. (Experimental conditions: 0.10 g L⁻¹ of photocatalyst, 30 mg L⁻¹ of RhB, 2.5mM of H₂O₂ and temperature = 25 ± 2 °C.); (b) Optimal pH = 3.5, UV-visible spectral changes of RhB at different time intervals.

Section S19. Effect of catalyst dosage

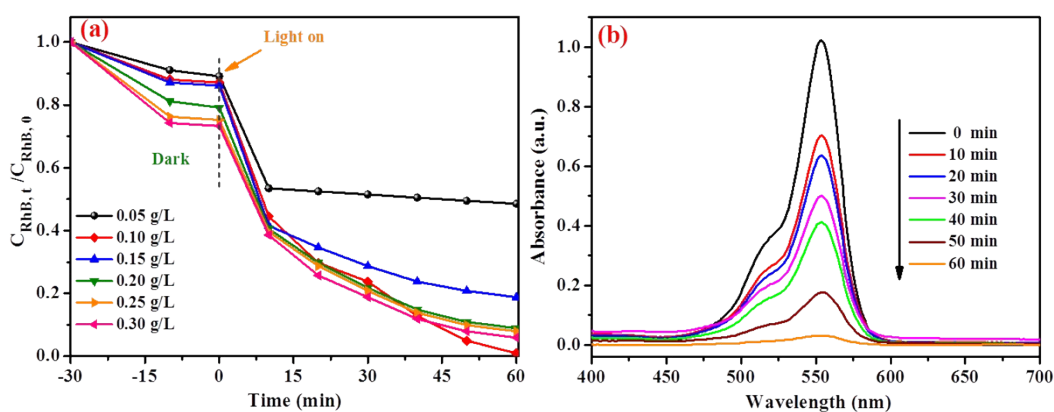


Fig. S13. (a) Effect of catalyst dosage on the degradation of RhB over FTU/H₂O₂/vis system. (Experimental conditions: 2.5 mM of H₂O₂, 30 mg L⁻¹ of RhB, pH of 3.5 and temperature = 25 ± 2 °C.); (b) Optimal [FTU]₀ = 0.10 g L⁻¹, UV-visible spectral changes of RhB at different time intervals.

Section S20. Effect of H₂O₂ concentration

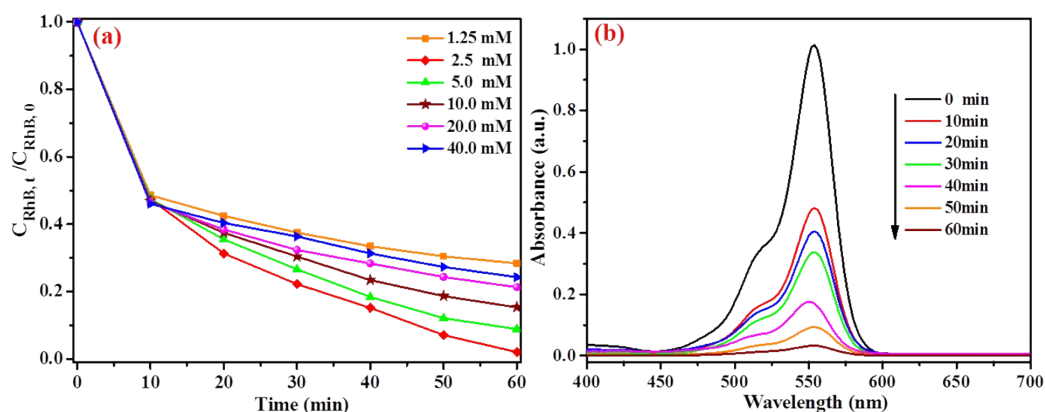


Fig. S14. (a) Effect of H₂O₂ concentration on the degradation of RhB over FTU/H₂O₂/vis system.

(Experimental conditions: 0.10 g L⁻¹ of FTU, 30 mg L⁻¹ of RhB, pH of 3.5 and temperature = 25 ± 2 °C.); (b) Optimal [H₂O₂]₀ = 2.5 mM, UV-visible spectral changes of RhB at different time intervals.

Section S21. Iron ion leached out detection and contributions of homogeneous and heterogeneous reactions

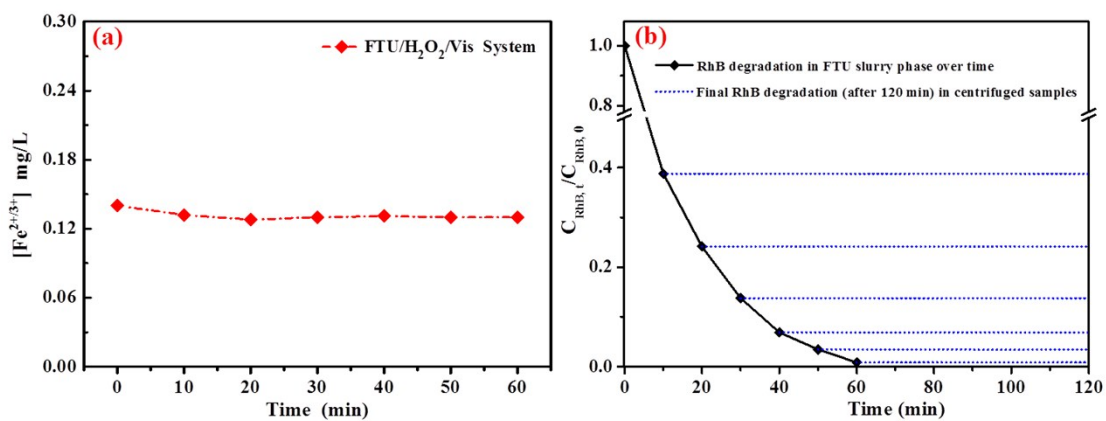


Fig. S15. (a) ICP detection of Fe ions leached out (0.06%) from FTU during the degradation process. (The average content of iron ions in the blank solution is about 0.13 mg/L) (b)

Contributions of homogeneous and heterogeneous reactions to the degradations of RhB.

Experimental conditions: [C_{RhB}]₀ = 30 mg L⁻¹, [FTU]₀ = 0.10 g L⁻¹, [H₂O₂]₀ = 2.5 mM, pH = 3.5 and

temperature = 25 ± 2 °C.

Section S22. Scavenge experiments

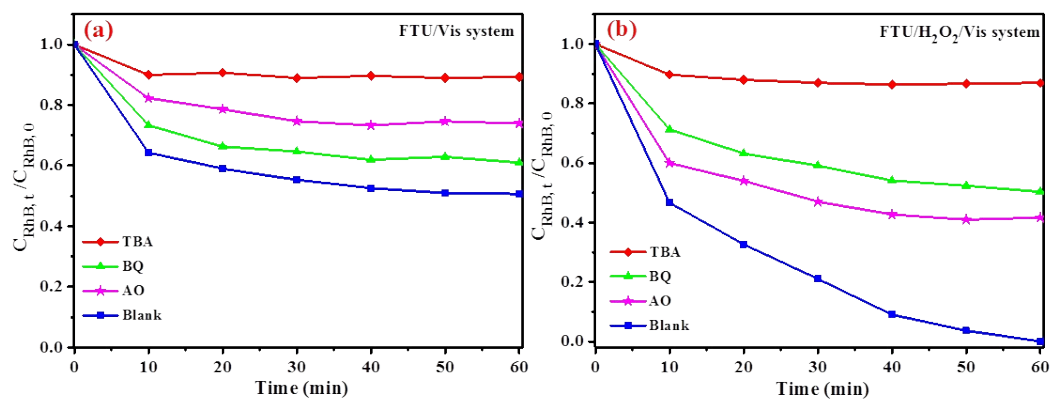


Fig. S16. Effects of different reactive species scavengers on the photo-degradations of RhB by the FTU composite (a) in the absence and (b) in the presence of H₂O₂ under visible-light irradiation.

Experimental conditions: $[C_{RhB}]_0 = 30$ mg L⁻¹, $[FTU]_0 = 0.10$ g L⁻¹, $[H_2O_2]_0 = 2.5$ mM, $[C_{TBA}]_0 = 5.4$ mM, $[C_{BQ}]_0 = 2.8$ mM and $[C_{AO}]_0 = 2.5$ mM, pH = 3.5 and temperature = 25 ± 2 °C.

Table S1

Heterogeneous photo-Fenton catalysis for removal of recalcitrant organic compounds.

No	Compound	Catalyst	Operational condition					Optimal performance	References
			[H ₂ O ₂]	[Cat]	pH	λ (nm)	T (°C)		
1	Rhodamine B [RhB] (10 mg/L)	Iron terephthalate metal-organic framework (MIL-53(Fe))	20 mM	0.4g/L	5.0	≥420	–	Completely decompose within 50 min	[7]
2	Methylene Blue [MB] (30 mg/L)	g-C ₃ N ₄ /NH ₂ -MIL-88B(Fe)	19.6mM	1 g/L	7.0	≥420	25	Almost Completely degradation within 120 min	[8]
3	Bisphenol A [BPA] (20 μM)	Goethite/ethylenediamine-N,N'-disuccinic acid (EDDS)	1.13mM	0.1 g/L Goethite, 0.1 mM EDDS	6.2	225-275	–	90% of BPA degradation within 12 h	[9]

4	Methylene Blue [MB] (0.0668m M)	Fe complexes MgAl-FeOx and MgAl-FeCit	3.34mM	0.1g/L	5.0	254	-	84% and 94% of MB degradation within 2 h using gAl-FeOx and MgAl-FeCit	[10]
5	orange I (20 mg/L)	Iron oxides	-	0.5g/L	5.25	365	-	TOC removal percentage optimal was 33.1% after 60 min	[11]
6	Rhodamine B [RhB] (30 mg/L)	Fe ^{III} -TCPPCl c UiO-66 [FTU]	2.5mM	0.1g/L	3.5	≥420	25	Completely decompose within 50 min	-

References:

1. T. Rhauderwiek, S. Waitschat, S. Wuttke, H. Reinsch, T. Bein and N. Stock, Nanoscale Synthesis of Two Porphyrin-Based MOFs with Gallium and Indium, *Inorg. Chem.*, 2016, **55**, 5312-5319.
2. L. Lin, C. Hou, X. Zhang, Y. Wang, Y. Chen and T. He, Highly efficient visible-light driven photocatalytic reduction of CO₂ over g-C₃N₄ nanosheets/tetra(4-carboxyphenyl)porphyrin iron(III) chloride heterogeneous catalysts, *Appl. Catal. B Environ.*, 2018, **221**, 312-319.

3. Y. Sun, L. Sun, D. Feng and H. C. Zhou, An In Situ One-Pot Synthetic Approach towards Multivariate Zirconium MOFs, *Angew. Chem. Int. Ed. Engl.*, 2016, **128**, 6581-6585.
4. C.-C. Su, M. Pukdee-Asa, C. Ratanatamskul and M.-C. Lu, Effect of operating parameters on the decolorization and oxidation of textile wastewater by the fluidized-bed Fenton process, *Sep. Purif. Technol.*, 2011, **83**, 100-105.
5. F. Chen, Q. Yang, X. Li, G. Zeng, D. Wang, C. Niu, J. Zhao, H. An, T. Xie and Y. Deng, Hierarchical assembly of graphene-bridged $\text{Ag}_3\text{PO}_4/\text{Ag}/\text{BiVO}_4$ (040) Z-scheme photocatalyst: An efficient, sustainable and heterogeneous catalyst with enhanced visible-light photoactivity towards tetracycline degradation under visible light irradiation, *Appl. Catal. B Environ.*, 2017, **200**, 330-342.
6. X. Li, Y. Pi, L. Wu, Q. Xia, J. Wu, Z. Li and J. Xiao, Facilitation of the visible light-induced Fenton-like excitation of H_2O_2 via heterojunction of g- $\text{C}_3\text{N}_4/\text{NH}_2$ -Iron terephthalate metal-organic framework for MB degradation, *Appl. Catal. B Environ.*, 2017, **202**, 653-663.
7. L. Ai, C. Zhang, L. Li and J. Jiang, Iron terephthalate metal – organic framework: Revealing the effective activation of hydrogen peroxide for the degradation of organic dye under visible light irradiation, *Appl. Catal. B Environ.*, 2014, **148-149**, 191-200.
8. X. Li, Y. Pi, L. Wu, Q. Xia, J. Wu, Z. Li and J. Xiao, Facilitation of the visible light-induced Fenton-like excitation of H_2O_2 via heterojunction of g- $\text{C}_3\text{N}_4/\text{NH}_2$ -Iron terephthalate metal-organic framework for MB degradation, *Appl. Catal. B Environ.*, 2017, **202**, 653-663.
9. W. Huang, M. Brigante, F. Wu, K. Hanna and G. Mailhot, Effect of ethylenediamine- $\text{N,N}'$ -disuccinic acid on Fenton and photo-Fenton processes using goethite as an iron source: optimization of parameters for bisphenol A degradation, *Environ. Sci. Pollut. Res.* 2013, **20**, 39-50.
10. Z. Huang, P. Wu, B. Gong, Y. Lu, N. Zhu and Z. Hu, Preservation of Fe complexes into layered double hydroxides improves the efficiency and the chemical stability of Fe complexes used as heterogeneous photo-Fenton catalysts, *Appl. Surf. Sci.*, 2013, **286**, 371-378.
11. J. Lei, C. Liu, F. Li, X. Li, S. Zhou, T. Liu, M. Gu and Q. Wu, Photodegradation of orange I in the heterogeneous iron oxide-oxalate complex system under UVA irradiation, *J. Hazard. Mater. B*, 2006, **137**, 1016-1024.